

Identifying and Correcting Pulse Breakup Errors from Freeway Loop Detectors

Ho Lee, PhD Candidate
Graduate Research Assistant
Department of Civil and Environmental Engineering and Geodetic Science
The Ohio State University
Columbus, OH 43210
E-mail: lee.2406@OSU.edu

Benjamin Coifman, PhD
Associate Professor
The Ohio State University
Joint appointment with the Department of Civil and Environmental Engineering and Geodetic Science,
and the Department of Electrical and Computer Engineering
Hitchcock Hall 470
2070 Neil Ave, Columbus, OH 43210
Phone: (614) 292-4282
E-mail: Coifman.1@OSU.edu

5,886 Words + 6 figures and tables = 7,386 words

Paper 11-1608

ABSTRACT

Loop detectors are the most common sensors used to collect freeway management data. There has been considerable research to screen the quality of loop detector data, but some significant detector errors have not received much attention due to the difficulty of identifying their occurrence. This paper examines one such error, pulse breakup: what should be a single pulse from a vehicle breaks up into two or more pulses because the detector momentarily drops out. We develop an algorithm to identify the presence of individual pulse breakup events. The algorithm is based on the nature of pulse breakup revealed from individual vehicle actuations with concurrent video ground truth. The algorithm begins with the comparison of the *on-times* from the two successive pulses bounding a given short *off-time*. To differentiate between pulse breakup and tailgating, the algorithm includes several comparisons of the adjacent on-times with respect to the ambient traffic conditions. A total of six steps are included in the algorithm. If two successive pulses satisfy all of the steps, these pulses are a suspected pulse breakup. Otherwise, these pulses are considered to arise from non-pulse breakup. The process is repeated over all pulses at each detector. The results can be used both to correct for the suspected pulse breakup events and the rate of suspected pulse breakup events provides an indication of the detector's health. The algorithm was tested over 68,281 actuations with concurrent video ground truth, in both free flow and congested conditions, from 15 detector stations (22 directional stations). As presented herein, the algorithm demonstrated good performance.

INTRODUCTION

Loop detectors are the most commonly used vehicle detector for automated surveillance in freeway management. They are effectively metal detectors embedded in the pavement. A typical loop detector station will have either one or two loop detectors per lane, i.e., single or dual loop detectors, respectively. Data obtained from loop detectors are used for applications such as ramp metering (1, 2), incident detection (3-5), travel time prediction (6, 7), and vehicle classification (8, 9). The performance of such applications greatly depends on the accuracy of the detector data, but data collected from loop detectors are prone to various errors caused by hardware and software problems. Detector errors degrade the quality of detector data, and the impact of these errors will propagate to subsequent measurements such as flow (the number of vehicles per unit time), occupancy (the percent time the detector is occupied), and speed from the loop detectors. In the end, data incorporating detector errors could affect the traffic control decisions and traveler information based on the detector's data.

There has been considerable research to screen the quality of loop detector data and to identify detector errors to improve data quality, both at the macroscopic and microscopic levels. Macroscopic tests embody the formalization of heuristics to check average measurements from a given sample period against statistical tolerance (10-13), while microscopic tests examine the individual vehicle actuations (14-18), when the loop detector turns "on" and "off" for each vehicle that passes over. However, some significant detector errors have not received much attention due to the difficulty of identifying their occurrence. This paper examines one such error, pulse breakup: a vehicle should register a single pulse per detector in its lane of travel but instead a detector momentarily drops out in the middle of the vehicle and produces two or more pulses.

Reviewing the literature to place our work in context, there are few if any macroscopic detector validation tests that explicitly seek to catch detectors exhibiting low to moderate pulse breakup rates; though, many of the macroscopic tests will catch a detector exhibiting a high pulse breakup rate simply because these detectors report an infeasibly high flow. Likewise, many of the existing microscopic tests may catch the secondary impacts of pulse breakup without explicitly looking for breakup events (e.g., the feasible range of headway and on-time, or cumulative distribution of vehicle lengths in (16)). There are two prior efforts that explicitly sought out pulse breakup events via microscopic data: Chen and May (14) use a threshold of the time gap (i.e., the off-time) and Cheevarunothai et al. (18) use the time headway between two successive pulses (i.e., the sum of a successive off-time and on-time). Both methods effectively use a short off-time as the indicator of a pulse breakup. While a pulse breakup usually results in a short off-time, a short off-time does not always correspond to pulse breakup because a short off-time can also arise due to tailgating and other vehicle maneuvers. Meanwhile, when traffic is congested, the resulting off-time in a pulse breakup will frequently exceed the static thresholds used by these tests to find pulse breakup events.

We develop an algorithm to identify the presence of individual pulse breakup events in both free flow and congested conditions. The algorithm is based on the nature of pulse breakup revealed from concurrent video recorded ground truth data. It begins with the comparison of on-times from the two successive pulses bounding a given short off-time, but then employs several heuristic comparisons of the adjacent on-times with respect to traffic conditions to refine the performance.

The remainder of this paper is organized as follows. First the procedure of collecting the ground truth data is presented. Followed by the characteristics of pulse breakup events revealed from the ground truth data. These characteristics are used to develop the pulse breakup detection algorithm. Next, the algorithm is evaluated with filed data from 15 detector stations (22 directional stations) with concurrent video ground truth data. Finally, the paper closes with conclusions.

GROUND TRUTH DATA

This study uses microscopic loop detector data with concurrent video ground truth to develop and validate an algorithm to identify the presence of individual pulse breakup events. The task of collecting and extracting the ground truth data consists of recording concurrent video of vehicle actuations from the loop detector, time synchronization between loop and video data, stepping through all of the loop detector actuations individually to review the video corresponding to a given loop detector actuation, and manually classify each detector actuation. A purpose built software graphical user interface (GUI) tool was developed in MATLAB to semi-automate the data reduction process. The GUI can step through the detector data in a given lane and display both the time series detector data for a few seconds before and after the given actuation along with the frame corresponding to the actuation time (this GUI was inspired by VideoSync (19)). If necessary, the user can step forward or backwards in time to review the video. From the direct comparison between concurrent detector and video data, the user indicates whether any errors were evident for the given actuation and if so, what the error was (pulse breakup; splashover - the erroneous detection in one lane of a vehicle from an adjacent lane; or other events such as a vehicle changing lanes). Once an actuation has been classified, the user clicks a button and the GUI jumps to the next detector actuation from that detector. The process was repeated for each visible lane during the entire time period with video data.

While our research examined all 65 loop detector stations in Columbus, Ohio, this paper only presents the results for stations that had concurrent ground truth data. The video data predominately came from the CCTV cameras recorded on a VCR in the Traffic Management Center, though in some cases a suitable view allowed for video recording in the field. The stations selected comprise the set that could be safely viewed. The specific dates and times were chosen arbitrarily to fit our availability, though in some cases prior to the video data collection we deliberately sought periods that typically exhibited recurring congestion. The detector stations include a mix of single and dual loop detectors. In the case of dual loop detectors this paper only analyzes the upstream detector, as if it were a single loop detector.

THE NATURE OF PULSE BREAKUP

Loop detectors record vehicle passages. When the detectors are operating properly the loop detector(s) in the given lane of travel should record each passing vehicle as a single pulse (comprised of a rising transition and a falling transition). Sometimes, however, a detector "drops out" in the middle of a vehicle then "flickers" back on before the vehicle has departed the detection zone, and thus, when such *pulse breakup* occurs, the vehicle is erroneously recorded as two or more pulses by the detector. Pulse breakup most often occurs when multiple unit vehicles (e.g., semi-trailer trucks or other vehicles pulling trailers) pass over a loop detector (18). These vehicles exhibit a sharp increase in the height above the detector (e.g., at the rear of the semi-tractor) or some other large effective drop in ferromagnetic presence (e.g., at the trailer tow-bar) somewhere in the middle of the multiple units. Conventional loop sensor cards use discrete thresholds to determine whether or not the loop detector is occupied by a vehicle. If the deviation in the middle of a multiple unit vehicle is large enough to exceed the turn-off threshold, the sensor card will erroneously report the detector as being unoccupied, i.e., the detector will dropout. Often the rear axles or other features on the trailer have sufficient ferromagnetic presence to cause the sensor card to subsequently turn back on and register another pulse. For example, Figure 1(a) shows the pulses over two seconds from all three lanes of a single loop detector station (station 9 northbound) as the detectors respond to vehicles. Without evaluation the two pulses from lane 2 would be recorded as two distinct vehicles. However, Figure 1(b) presents a concurrent frame from the video, showing that the two pulses in lane 2 both came from the same semi-trailer truck passing over the loop detector. For scale reference, a car is evident in lane 3 immediately behind the truck in both the plot and the image.

Figure 1(c) shows a hypothetical example of a semi-trailer truck's actuation breaking up into two pulses; both in the time-space diagram and as recorded in the time-series detector data. The unobserved, actual on-time (OnT^A) denotes the period when the loop detection zone was physically occupied by the truck. But because of the pulse breakup in the recorded data OnT^A is divided into two distinct on-times (OnT_1 and OnT_2) and one off-time ($OffT_1$). The schematic on the left of the plot shows the truck's tractor and trailer at the instant the tractor leaves the detection zone. The separate parts of the semi-trailer truck associated with the on-times and off-time are labeled on the plot. Initially the ground clearance of a typical semi-trailer truck is relatively small, the tractor is close to the ground (L_1^P , contributed to OnT_1), and then rises significantly under the trailer (L_x^P , contributed to $OffT_1$), only to come close to the ground once more with the trailer's axles (L_2^P , contributed to OnT_2). Given a vehicle's speed (V), the on-times and off-time in a pulse breakup can be expressed via Equation 1.

$$\begin{aligned} OnT_1 &= \frac{L_1^P + DZ}{V} = \frac{L_1}{V} \\ OnT_2 &= \frac{L_2^P + DZ}{V} = \frac{L_2}{V} \\ OffT_1 &= \frac{L_x^P - DZ}{V} = \frac{L_x}{V} \end{aligned} \quad (1)$$

If the pulse breakup error goes undetected, OnT_1 and OnT_2 will appear to be two short vehicles separated by the relatively brief $OffT_1$. It is clear that this error causes flow to be too high and occupancy to be too low. If the on-times are used to measure or estimate vehicle length, the resulting lengths from the two pulses (at best, L_1 and separately L_2) do not correspond to the vehicle's actual effective length ($L_1 + L_2 + L_x$), thus degrading the performance of any subsequent length based vehicle classification using the detector's data. The pulse breakup can also impact the speed estimate/measurement.

DEVELOPMENT OF THE PULSE BREAKUP DETECTION ALGORITHM

We develop a pulse breakup detection algorithm to identify most pulse breakup events in the microscopic, vehicle actuation pulse train. The method is based on the nature of pulse breakup events revealed from the ground truth data. The development dataset consists of 2 hrs of free flow data from the three northbound lanes at station 9 on June 5, 2006. A total 306 out of 7,243 vehicles (4%) exhibit pulse breakup and all observed pulse breakup events consist of two pulses (we rarely observed a vehicle breaking up into more than two pulses in the ground truth datasets, so given the lack of empirical data we were unable to explicitly test these conditions). Like the earlier work (14, 18), we begin with a simple off-time threshold, but then employ five heuristic comparisons of the adjacent on-times with respect to traffic conditions to separate the breakup events from the non-breakup events. The five heuristics are:

- Dynamic off-time
- Ratio of on-times
- Ratio of off-time and preceding on-time
- 20th percentile off-time
- Maximum vehicle length

as defined in the following subsections. The method is designed to work at both single loop detectors and individually at each loop in dual loop detectors, as such, it only uses metrics that can be collected at single loop detectors (the method can easily be extended to use measured speed from dual loop detectors, as shown in (20)).

Dynamic Off-time

Figure 2(a) shows the cumulative distribution function (CDF) of off-times from pulse breakup events and non-pulse breakup events. During free flow a static off-time threshold, $OffT_{FF_Threshold}$, of 20/60 seconds does a good job of selecting pulse breakup events (100% of the pulse breakup events have off-times less than or equal to 20/60 seconds), while catching only 110 false positives from the 7,248 valid actuations (1.5%). Although not perfect, such a clean distinction is lost in congestion, many pulse breakup events exhibit off-times in excess of the static time threshold. Instead, we use a static length; given $OffT_{FF_Threshold}$, the free speed, V_f , and size of the detection zone, DZ , from Figure 1(c) there is some maximum physical gap, L_X^P that will be labeled as suspected of arising from pulse breakup, as per Equation 2.

$$L_X^P = V_f \times OffT_{FF_Threshold} + DZ \quad (2)$$

At some congested speed, V_c , this L_X^P will correspond to a larger off-time threshold, $OffT_{C_Threshold}$, via Equation 3.

$$OffT_{C_Threshold} = \frac{L_X^P - DZ}{V_c} \quad (3)$$

This dynamic off-time threshold can be rewritten as Equation 4.

$$OffT_{C_Threshold} = \frac{V_f}{V_c} \times OffT_{FF_Threshold} \quad (4)$$

In other words, the off-time threshold from L_X^P in congestion corresponds to the free flow off-time threshold multiplied by the ratio V_f/V_c . As one would expect, the off-time threshold in congestion is greater than in free flow because $V_f/V_c > 1$. A given vehicle's speed at a single loop detector is estimated from the assumed effective vehicle length, \tilde{L} , divided by median on-time (21) in a window of 41 pulses (the present study uses a window centered on the subject pulse, but some real-time applications may require the window to end with the subject pulse; although not shown, we tested this alternative and found similar results). As shown in (21), the median on-time yields more accurate estimates than conventional single loop speed estimates. Meanwhile, we estimate V_f over the period 9 hr to 15 hr on a single day, though in practice, to avoid the impact of transient events one would likely want to use the median V_f from several recent days. In any event, $OffT_{C_Threshold}$ can be rewritten as Equation 5,

$$\begin{aligned} OffT_{C_Threshold} &= \frac{\frac{\tilde{L}}{\text{median}(\text{on-times})_{\text{off-peak time period}}}}{\frac{\tilde{L}}{\text{median}(\text{on-times})_{41\text{pulses}}}} \times OffT_{FF_Threshold} \\ &= \frac{\text{median}(\text{on-times})_{41\text{pulses}}}{\text{median}(\text{on-times})_{\text{off-peak time period}}} \times OffT_{FF_Threshold} \end{aligned} \quad (5)$$

where we use "OnT" and "OffT" to denote a single on-time or off-time, respectively, and "on-times" in the equations to denote a set of several OnT. Since the threshold in Equation 5 depends on the prevailing traffic speed, we call it the "dynamic off-time". An OffT is suspect if it is less than the threshold, rewriting the equation as such a test yields Equation 6.

$$\frac{\text{OffT}}{\text{median (on-times)}_{41 \text{ pulses}}} \leq \frac{\text{OffT}_{\text{FF_Threshold}}}{\text{median (on-times)}_{\text{off-peak time period}}} \quad (6)$$

Ratio of On-times

Most of the observed pulse breakup events arose in the middle of semi-trailer trucks, between the tractor and rear axles. So from Equation 1, OnT_1 and OnT_2 in Figure 1(c) should be proportional to the length of the tractor and the trailer axles, respectively. The effective length observed for the tractor is typically longer than the effective length of trailer axles, e.g., about 99% of the pulse breakup events in the development data had OnT_1 larger than OnT_2 . Capturing this observation in a metric, the ratio of on-times is used to select successive pulses that exhibit this relationship. Like the dynamic off-time above, the ratio is used rather than the difference because the ratio of on-times is impacted less by traffic speed, as will be discussed below. Assuming the vehicle speed is roughly constant between OnT_1 and OnT_2 , from Equation 1, the ratio of two successive on-times is related to the ratio of the corresponding effective vehicle length via Equation 7.

$$\frac{\text{OnT}_2}{\text{OnT}_1} = \frac{\frac{L_2}{V_2}}{\frac{L_1}{V_1}} \approx \frac{L_2}{L_1} \quad (7)$$

Figure 2(b) shows the CDFs of the on-time ratio from Equation 7 for pulse breakup events and separately for successive non-pulse breakup events in the development dataset. We seek to use Equation 7 to differentiate between pulse breakup and non-pulse breakup events using a threshold. While a threshold of 1 would capture 99% of the pulse breakup events, it would also capture 50% of the non-pulse breakup events. To establish the on-time ratio threshold, we seek the point where the difference between the two CDFs is largest. Figure 2(c) shows the difference between the two CDFs over the range from 0 to 2.5 at steps of 0.01. The peak is observed at 0.72 and we take this as the threshold for the on-time ratio test, yielding Equation 8,

$$\frac{\text{OnT}_2}{\text{OnT}_1} \leq 0.72 \quad (8)$$

Of course the on-time ratio test is not meant to be applied alone. Figure 2(d) shows a scatter plot of intervening off-time versus on-time ratio for the pulse breakup events in the development dataset. The vertical dashed line shows the threshold of 0.72 from Equation 8 and horizontal line shows the threshold of 20/60 seconds from Equation 6 (since these data come from free flow, the dynamic off-time threshold would remain around 20/60 seconds for these data.). Roughly 94% (289 out of 306) of the pulse breakup events fall in the lower left quadrant, while only 0.1% (7 out of 7,248) of the non-pulse breakup events (not shown) fall in this same quadrant. Among the pulse breakup events there were 8 single unit trucks pulling trailers, shown in Figure 2(d) with a different symbol than the multiple unit trucks. Most of the single unit trucks pulling trailers exceed the on-time ratio threshold, but these vehicles typically exhibit a much shorter off-time (all below 10/60 seconds) compared to the multiple unit trucks with pulse breakup. From the concurrent video, the pulse breakup events from single unit trucks pulling trailers occur at the trailer hitch, i.e., the smallest cross-section of the vehicle; however, the pulse breakup events from the multiple unit trucks typically occur at the end of the tractor, when the ground clearance suddenly increases. If in addition to those successive on-times falling in the lower left quadrant of Figure 2(d),

selecting all points that fall below a threshold of 6/60 seconds in Equation 6 (i.e., ignoring the on-time ratio while employing a more stringent off-time threshold), 50% of the pulse breakup events falling outside the quadrant are also caught. Moreover, since the smallest off-time from the non-pulse breakup data in this set is 8/60 seconds, the additional condition does not increase the number of non-pulse breakup events erroneously selected.

Ratio of Off-time and Preceding On-time

For the observed pulse breakup events, the on-time of the preceding pulse (OnT_1) is generally greater than the off-time ($OffT_1$). Assuming the vehicle speed is roughly constant between OnT_1 and $OffT_1$, from Equation 1, the ratio can be expressed via Equation 9,

$$\frac{OffT_1}{OnT_1} = \frac{L_x}{L_1} = \frac{L_x^p - DZ}{L_1^p + DZ} \quad (9)$$

As with the on-time ratio, Equation 9 just depends on the physical characteristics of the vehicle, not the traffic speed. Like the on-time ratio test, Figure 2(e) shows the CDFs of the ratio of off-time and preceding on-time from Equation 9 for pulse breakup events and separately for successive non-pulse breakup events in the development dataset. We set the threshold ratio of off-time and preceding on-time at the point where the difference between the two CDFs is largest. Figure 2(f) shows the difference between the two CDFs over the range from 0 to 2.5 at steps of 0.01. The peak is observed at 1.2 and we take this as the threshold for the ratio of off-time and preceding on-time test, yielding Equation 10,

$$\frac{OffT_1}{OnT_1} \leq 1.2 \quad (10)$$

20th Percentile Off-time

From Equation 6, the dynamic off-time in congestion depends on the median on-time over 41 successive pulses, centered on the current pulse. Usually speeds are stable enough for this constraint to hold, but under heavy congestion, speeds can change by more than 100% over a sample of 41 pulses. So, the median on-time over 41 successive pulses is sometimes larger than the microscopic traffic condition would dictate for the given vehicle. The large threshold of off-time due to large median on-time is more likely to erroneously select non-pulse breakup events and mark them as suspected pulse breakup events. To accommodate these errors, we exploit the fact that the off-time in a pulse breakup is usually shorter than the off-time between two successive vehicles. Or formalizing it in terms of a rule, the off-time in a suspected pulse breakup should fall within the lowest 20% of off-times observed in the 41 successive pulses, via Equation 11,

$$OffT_1 \leq P_{20}(\text{off-times})_{41 \text{ pulses}} \quad (11)$$

Maximum Vehicle Length

When a pulse breakup occurs, using the notation in Figure 1(c), OnT^A should be at least equal to the sum of OnT_1 , OnT_2 and $OffT_1$, denoted OnT^{sum} . For each suspected pulse breakup event that has passed all of the preceding tests, the product of estimated speed and OnT^{sum} yields an estimated vehicle length in the absence of a pulse breakup, i.e., as if $OffT_1$ never occurred. If the estimated vehicle length from OnT^{sum} is shorter than the maximum possible vehicle length, the event remains suspect of pulse breakup. Otherwise, if the resulting estimated vehicle length exceeds the maximum possible vehicle length, e.g., a short vehicle tailgating a long vehicle, the event is no longer suspected of pulse breakup. Formalizing the test, a suspected pulse breakup is retained if Equation 12 is met and discarded otherwise.

$$\frac{\tilde{L}}{\text{median}(\text{on-times})_{41 \text{ pulses}}} \times \text{OnT}^{\text{sum}} \leq L_{\text{Threshold}} \quad (12)$$

To set maximum possible vehicle length, $L_{\text{Threshold}}$, we examined the effective vehicle length measured from dual loop detectors. The maximum observed length is usually less than 85ft. However, a long vehicle's estimated length could be slightly longer than its actual length if the long vehicle's speed in free flow traffic is slightly below the median speed. The median speed is expected to come from a passenger vehicle (21) but some locations have a different speed limit for trucks and passenger cars, while in other locations passenger cars may be more likely to speed than trucks. So $L_{\text{Threshold}}$ is set to a conservative value of 100 ft, corresponding to an 85 ft long vehicle traveling at 55 mph but with speed overestimated at 65 mph.

The Pulse Breakup Detection Algorithm

Combining all of these tests into an algorithm to differentiate between pulse breakup events and non-pulse breakup events, Figure 3 shows the flowchart of the algorithm. To make the flowchart more intuitive, we replace OnT_1 , OnT_2 and OffT with their relative descriptions within the given pair of pulses: "preceding on-time", "following on-time" and "off-time", respectively. If two successive pulses satisfy all of the checks, these pulses are suspected of pulse breakup, otherwise, these pulses are considered to be from separate vehicles and no pulse breakup is suspected between the pair. The process is repeated over all successive pulses from each detector.

The result can be used to correct suspected pulse breakup events, e.g., the two pulses can be combined (OnT^{sum}) as an estimate of OnT^{A} both to improve the accuracy of the on-time and the vehicle count. Furthermore, as will be discussed below, the frequency of suspected pulse breakup events can be used as an indicator of the detector health, e.g., dispatching a technician to a detector with a high frequency of suspected pulse breakup events to fix the underlying hardware fault and thus, eliminate both the detected and undetected pulse breakup events.

EVALUATION OF THE ALGORITHM

Application and Results

Approximately 18 hours of directional traffic data were ground truthed from 31 different datasets collected at 22 different directional detector stations. A total of 68,281 detector actuations were manually ground truthed (in the absence of a detector error, there should be exactly one actuation per vehicle). Of the 31 datasets, 22 are from free flow, comprising 8.3 hr from 10 directional stations with pulse breakup (including the one development set) and 5.2 hr from 12 directional stations without pulse breakup. The remaining nine datasets are from congestion, including 2.3 hr from four directional stations with pulse breakup and 2.3 hr from five directional stations without pulse breakup.

None of the datasets with pulse breakup suffered from splashover, but seven of the sets without pulse breakup did exhibit splashover in one or more detector. The non-vehicle pulses from the splashover errors yield many more short off-times in the pulse train, some of which will be retained as suspected pulse breakup events. To avoid such confounding errors, the detectors with splashover are excluded from further analysis in this paper. Fortunately the splashover errors severe enough to lead to confounding errors can be detected using a separate algorithm, (22), and if a detector is suspected of splashover by (22), we recommend first correcting the splashover error before acting on the results from the pulse breakup algorithm.

The performance of the algorithm is summarized in Table 1. The first few rows show the results from the development data, while the rest of the table shows the results for the evaluation datasets,

excluding the development data. The evaluation data are grouped by free flow and congested sets, and within each group the results are presented separately for the detectors with and without pulse breakup (while space constraints preclude presentation here, the results for each individual dataset are presented in (20), including the detectors with splashover errors). The total pulses column tallies the number of pulses recorded by the detector during the video data collection. The actual pulse breakup column tallies the number of pulse breakup events seen from the ground truth data, while the suspected pulse breakup column tallies the number of events labeled by the algorithm as being pulse breakup events. The success column counts the number of times that the algorithm correctly caught an actual pulse breakup, while the false positive column counts the number of times that the algorithm erroneously labeled a non-pulse breakup as a suspected pulse breakup event (as shown in the last few columns, the ground truth revealed that these errors were due to tailgating and lane change maneuvers, LCM). Any actual pulse breakup events that were not included in the success column are counted in the false negative column, i.e., the algorithm failed to catch the given pulse breakup event.

During free flow, at the detectors with pulse breakup events the algorithm successfully caught 384 out of 416 of the events (92.3%), which is just below the performance seen on the development data (95.8%). These 384 events represent 1.46% of the total number of pulses. In contrast, the algorithm had 33 false positives among the detectors without pulse breakup events, representing 0.27% of the pulses at these detectors. In other words, the success rate at the detectors with pulse breakup (1.46%) is more than five times larger than the false positive rate at the detectors without (0.27%). The contrast is slightly higher when comparing the algorithm output, i.e., the suspected pulse breakup rate.

During congestion, the algorithm correctly catches 157 out of 169 pulse breakup events (92.9%), comparable to the free flow performance. The success rate is slightly higher than free flow, correctly catching 1.58% of the total pulses, but the false positive rate at the detectors without pulse breakup events has increased by a factor of four in congestion (1.02%) compared to free flow. False positives are much more frequent in congested conditions due to our dynamic definition of tailgating. A false positive error due to tailgating indicates that the physical gap between two vehicles is under 38 ft, the maximum distance of L_x^p . In congested conditions one should expect to see shorter physical gaps between two successive vehicles due to the lower speeds and this fact is reflected in the higher rate of false positive errors. Not all vehicles with physical gap under 38 ft result in false positive errors, since the remaining tests in the algorithm will still successfully eliminate many of these cases.

Based on these results, during free flow the algorithm appears beneficial for differentiating between detectors with and without pulse breakup events. When congestion sets in, the algorithm continues to yield benefits at detectors with pulse breakup (as identified during free flow periods) but the increased rate of false positives at detectors without pulse breakup events begins to outweigh the benefits. Taking a conservative path, the algorithm should be suppressed in congestion if there is little evidence of pulse breakup during free flow at a detector.

Defining the Suspected Pulse Breakup rate (SPBUr) and the Actual Pulse Breakup rate (APBUr) for each detector via Equation (13), among the free flow datasets 29 detectors exhibited pulse breakup (APBUr > 0) and 34 did not. Seven of the detectors had APBUr > 4%, the largest being 7.2%. Using a threshold of SPBUr > 1% during free flow to flag a detector as being suspected of a chronic pulse breakup problems, this threshold would exclude 33 of 34 detectors without pulse breakup, 10 of 10 detectors with APBUr < 1%, and it would catch 17 of 19 detectors with APBUr > 1%. The sample size was limited to the period with ground truth at the given detector. Performance would likely improve when using a longer period. One of the detectors with APBUr > 1% that was missed was a little used lane, with only 83 pulses and a single pulse breakup event. The other detector that was missed had an APBUr of 1.22% but a SPBUr of 0.89%.

$$\begin{aligned}
 \text{SPBU}_r &= \frac{\text{Number of suspected pulse breakups}}{\text{Number of pulses}} \\
 \text{APBU}_r &= \frac{\text{Number of actual pulse breakups}}{\text{Number of pulses}}
 \end{aligned}
 \tag{13}$$

To test the diagnostic power of this test, we selected two detector stations with many suspected pulse breakup events and asked the operating agency (the Ohio Department of Transportation) to increase the detector sensitivity setting of all loop detectors in both directions at both stations. A second round of video data was collected for each station in both directions. Before the change we saw 499 pulse breakup events out of 21,983 pulses (2.27%) and no splashover events from the 14 detectors at the two stations. After the change we saw no pulse breakup events over 8,782 pulses, though one detector now exhibited 68 splashover events out of 2,434 pulses (2.79%), indicating an overcompensation at that detector (obviously, an increase in detector sensitivity should reduce the occurrence of pulse breakup, while increasing the likelihood of splashover and related errors). All of these data come from free flow. The before data are included in Table 1, while the after data are not (further details of this diagnostic comparison can be found in (20)).

Sensitivity of the Algorithm to the Choice of Threshold Values

There are several parameters in the algorithm to identify pulse breakup that were derived from one detector station, using only the 2 hr long development set. The preceding results are based on the assumption that the nature of pulse breakup events observed at the development location is similar to all of the detector stations. While it is not possible to test detectors for which we do not have data, this section examines the optimal thresholds for (I) *ratio of off-time and preceding on-time*, and (II) *ratio of on-times* in the algorithm, using the entire free flow evaluation dataset with pulse breakup (i.e., excluding the development set). Concurrently varying both ratios, Figure 4 shows the resulting performance. The ratio of off-time and preceding on-time is varied from 0.7 to 1.5 at increments of 0.1, separated by the bold vertical dashed lines. Between each pair of bold dashed lines, the on-time ratio is varied between 0.69 and 0.78 at increments of 0.01. In total 90 combinations are tested. The plot shows the number of false positives, false negatives, and the sum of the two errors. The sum is minimized for two off-time ratio threshold values, 1.2, when the on-time ratio is between 0.72 and 0.76 (except 0.74), and 1.3, when the on-time ratio is between 0.71 and 0.75 (except 0.74). The original off-time ratio of 1.2 and on-time ratio of 0.72 from the calibration dataset falls within this range. These results suggest that the calibration from one location is indeed transferable to the other locations in this study. Though it is possible that these results may still exhibit biases that are common across the entire Columbus Metropolitan Freeway Management System, so if such microscopic event data become available from other metropolitan areas, it would be advisable to test the calibration on those facilities as well.

A Comparison of Algorithm Performance

Finally, we compare the performance of two earlier pulse breakup detection algorithms against our algorithm [L&C] using the evaluation datasets. All three of the algorithms are compatible with single loop detectors. In the previous algorithms, Chen and May (14), [C&M], used a static threshold of the time gap (i.e., the off-time between two successive pulses) of 15/60 seconds, while Cheeverunothai et al. (18), [CYN], used a static threshold of the time headway (the sum of a successive off-time and on-time) of 38/60 seconds. Both algorithms considered two successive pulses as a suspected pulse breakup if the metric (off-time for C&M or the time headway for CYN) is below the given threshold. The performance of each algorithm is evaluated in terms of the number of success, false positive, and false negative, summed across all of the detectors with ground truth data, as shown in Table 2.

For detectors with pulse breakup in free flow conditions, the success column shows that our algorithm caught 36% more pulse breakup events than C&M, and 38% more than CYN. As a direct

result, our false negative rate was smaller, on the order of one quarter the size of either of the earlier methods. Our false positive rate was 1/6 of C&M and 1/60 of CYN. For detectors without pulse breakup in free flow conditions, our false positive rate was 35% of C&M and 8% of CYN. For detectors with pulse breakup in congested conditions, our algorithm caught more than three times as many pulse breakup events than C&M and more than 10 times as many as CYN. As a direct result, our false negative rate was an order of magnitude smaller in size compared to either of the earlier methods. Our false positive rate was roughly 5 times larger than C&M and identical to CYN. Compared to C&M, the 18 extra false positives by our algorithm is much smaller than the 108 extra successes. For detectors without pulse breakup in congested conditions, our false positive rate was 39% larger than C&M and 15% larger than CYN.

CONCLUSIONS

This paper developed and tested an algorithm to identify pulse breakup events from individual vehicle actuation data. The algorithm started with the comparison of on-times from the two consecutive pulses bounding a given short off-time, and it improves the distinction between pulse breakup and non-pulse breakup events via several heuristic tests of the adjacent on-times with respect to the ambient traffic conditions. The algorithm for pulse breakup was tested over 15 detector stations (22 directional stations) with concurrent video-recorded ground truth data. Overall, 68,281 actuations in both free flow and congested conditions were tested and 834 out of 891 (94%) actual pulse breakups were correctly identified as pulse breakup. The algorithm correctly caught over 92% of pulse breakup events under each condition tested in the evaluation datasets. In free flow traffic the success rate at detectors with pulse breakup is about five times larger than the false positive rate at detectors without pulse breakup. In congestion the algorithm remains beneficial at the detectors with pulse breakup but the false positive rate increases at the non-pulse breakup detectors. So it may be better to suppress the algorithm at a given detector during congestion if there is little evidence of pulse breakup at the detector during free flow. We found using a threshold of 1% on SPBUr did a good job of selecting detectors with APBUr over 1% while excluding most non-pulse breakup detectors. The algorithm was compared against two previous algorithms and our work exhibited a higher success rate, lower total false positive rate, and lower false negative rate compared to the earlier algorithms.

The pulse breakup detection algorithm could lead to a very inexpensive means to improve the quality of loop detector data at existing loop detector stations. After further refinement, in the short term the algorithm could be incorporated into a field diagnostic tool to assess the performance of a given station. In the longer run, the test should be incorporated into the standard controller software so that the controller can continually assess the health of the detectors.

ACKNOWLEDGEMENTS

This material is based upon work supported in part by NEXTRANS the USDOT Region V Regional University Transportation Center and by the California PATH (Partners for Advanced Highways and Transit) Program of the University of California, in cooperation with the State of California Business, Transportation and Housing Agency, Department of Transportation. The Contents of this report reflect the views of the authors who are responsible for the facts and accuracy of the data and results presented herein. The contents do not necessarily reflect the official views or policies of the State of California. This report does not constitute a standard, specification or regulation.

The authors are grateful for the help of the Ohio Department of Transportation in facilitating this research.

REFERENCES

- [1] Papageorgiou, M., H. Hadj-Salem, and F. Middleham. ALINEA Local Ramp Metering Summary of Field Results. In *Transportation Research Record: Journal of the Transportation Research Board*, No. 1603, Transportation Research Board of the National Academies, Washington, D.C., 1997, pp. 90-98.
- [2] Hourdakakis, J. and P. G. Michalopoulos. Evaluation of Ramp Control Effectiveness in Two Twin Cities Freeways. In *Transportation Research Record: Journal of the Transportation Research Board*, No. 1811, Transportation Research Board of the National Academies, Washington, D.C., 2002, pp. 21-29.
- [3] Payne, H. J. and S. C. Tignor. Freeway Incident-Detection Algorithms Based on Decision Trees with States. In *Transportation Research Record: Journal of the Transportation Research Board*, No. 682, Transportation Research Board of the National Academies, Washington, D.C., 1978, pp. 30-37.
- [4] Payne, H. J. and S. M Thompson. *Development and Testing of Operational Incident Detection Algorithms: technical report*, U.S. Federal Highway Administration, 1997
- [5] Williams, B.M. and A. Guin. Traffic Management Center Use of Incident Detection Algorithms: Findings of a Nationwide survey. *IEEE Transactions on intelligent transportation systems*, Vol. 8, No. 2, 2007, pp. 351-358.
- [6] Kwon, J., B. Coifman, and P. Bickel. Day-to-Day travel time trends and travel time prediction from loop detector data. In *Transportation Research Record: Journal of the Transportation Research Board*, No. 1717, Transportation Research Board of the National Academies, Washington, D.C., 2000, pp. 120-129.
- [7] Coifman, B. and S. Krishnamurthy. Vehicle Reidentification and Travel Time Measurement Across Freeway Junctions Using the Existing Detector Infrastructure. *Transportation Research: Part C*, Vol. 15, No. 3, 2007, pp. 135-153.
- [8] *Traffic Monitoring Guide*. Federal Highway Administration, 2001.
- [9] Coifman, B. and S. Kim. Speed Estimation and Length Based Vehicle Classification from Freeway Single Loop Detectors. *Transportation Research: Part C*, Vol. 17, No. 4, 2009, pp. 349-364.
- [10] Jacobson, L., N. Nihan, and J. Bender. Detecting Erroneous Loop Detector Data in a Freeway Traffic Management System. In *Transportation Research Record: Journal of the Transportation Research Board*, No. 1287, Transportation Research Board of the National Academies, Washington, D.C., 1990, pp. 151-166.
- [11] Cleghorn, D., F. Hall, and D. Garbuio. Improved Data Screening Techniques for Freeway Traffic Management Systems. In *Transportation Research Record: Journal of the Transportation Research Board*, No. 1320, Transportation Research Board of the National Academies, Washington, D.C., 1991, pp. 17-23.
- [12] Turochy, R.E. and B. L. Smith. New Procedure for Detector Data Screening in Traffic Management Systems. In *Transportation Research Record: Journal of the Transportation Research Board*, No. 1727, Transportation Research Board of the National Academies, Washington, D.C., 2000, pp. 127-131.

- [13] Chen, C., J. Kwon, J. Rice, A. Skabardonis, and P. Varaiya. Detecting Errors and Imputing Missing Data for Single Loop Surveillance Systems. In *Transportation Research Record: Journal of the Transportation Research Board*, No. 1855, Transportation Research Board of the National Academies, Washington, D.C., 2003, pp. 160-167.
- [14] Chen, L. and A. D. May. Traffic Detector Errors and Diagnostics. In *Transportation Research Record: Journal of the Transportation Research Board*, No. 1132, Transportation Research Board of the National Academies, Washington, D.C., 1987, pp. 82-93.
- [15] Coifman, B. Using Dual Loop Speed Traps to Identify Detector Errors. In *Transportation Research Record: Journal of the Transportation Research Board*, No. 1683, Transportation Research Board of the National Academies, Washington, D.C., 1999, pp. 47-58.
- [16] Coifman, B. and S. Dhoorjaty. Event Data Based Traffic Detector Validation Tests. *ASCE Journal of Transportation Engineering*, Vol. 130, No. 3, 2004, pp. 313-321.
- [17] Coifman, B. and H. Lee. A Single Loop Detector Diagnostic: Mode On-Time Test. *Proc. of Applications of Advanced Technology in Transportation*, ASCE, August 13-16, 2006, Chicago, IL. pp. 623-628.
- [18] Cheevarunothai, P., Y. Wang, and N. L. Nihan. Using Dual-Loop Event Data to Enhance Truck Data Accuracy. In *Transportation Research Record: Journal of the Transportation Research Board*, No. 1993, Transportation Research Board of the National Academies, Washington, D.C., 2007, pp. 131-137.
- [19] Caltrans, 2007. *VideoSync*. <http://www.dot.ca.gov/newtech/operations/videosync/index.htm> Accessed January 3, 2010.
- [20] Lee, H. *Algorithms to Identify Splashover and Pulse Breakup Errors from Freeway Loop Detector Data*. Ph.D. dissertation. The Ohio State University, anticipated Spring, 2011.
- [21] Coifman, B., S. Dhoorjaty, and Z. Lee. Estimating Median Velocity Instead of Mean Velocity at Single Loop Detectors. *Transportation Research: Part C*, Vol 11, No 3-4, 2003, pp. 211-222.
- [22] Lee, H. and B. Coifman. An Algorithm to Identify Splashover Errors at Freeway Loop Detectors. (*in review*).

LIST OF TABLES

TABLE 1 Summary of the performance of the pulse breakup detection algorithm during free flow and congested conditions. The first rows present the development dataset, while the remaining rows present the evaluation datasets.

TABLE 2 Comparison of our proposed algorithm against two previous algorithms for detecting pulse breakup events.

LIST OF FIGURES

FIGURE 1 (a) A plot of transition pulses with pulse breakup recorded at station 9 northbound, (b) a concurrent video frame showing the two vehicles that gave rise to the three pulses, and (c) a time-space diagram illustrating a hypothetical example of pulse breakup and the associated detector's response.

FIGURE 2 From the development dataset at station 9 northbound, (a) CDF of off-times from pulse breakup and from non-pulse breakup events, (b) CDF of the on-time ratio from pulse breakup and from non-pulse breakup events, (c) the difference between the two CDFs of the on-time ratio, (d) a scatter plot of off-time versus on-time ratio in pulse breakup events, (e) CDF of the ratio of off-time and preceding on-time from pulse breakup and from non-pulse breakup events, and (f) the difference between the two CDFs of the ratio of off-time and preceding on-time.

FIGURE 3 A flowchart of the algorithm to identify pulse breakup from single loop detectors.

FIGURE 4 Sensitivity analysis of the performance of the pulse breakup detection algorithm relative to the combination of the on-time ratio threshold, and the ratio of off-time and preceding on-time threshold. The bold vertical delineations show the transition from one ratio of off-time and preceding on-time threshold to the next (indicated with large numbers on the figure), while the lighter vertical delineations show the steps between on-time ratio thresholds (indicated along the horizontal axis).

TABLE 1 Summary of the performance of the pulse breakup detection algorithm during free flow and congested conditions. The first rows present the development dataset, while the remaining rows present the evaluation datasets

Types	Traffic condition	Data Set	Total pulses	Actual pulse breakup	Suspected pulse breakup	Performance			Reason of false positive	
						Success	False positive	False negative	Tail-gating	LCM
Development	Free flow	With pulse breakup	7,563	306	296	293	3	13	2	1
			Percent of pulses	4.05%	3.91%	3.87%	0.04%	0.17%	-	-
			Percent of pulse breakups	-	-	95.8%	-	-	-	-
Evaluation	Free flow	With pulse breakup	26,230	416	397	384	13	32	10	3
			Percent of pulses	1.59%	1.51%	1.46%	0.05%	0.12%	-	-
			Percent of pulse breakups	-	-	92.3%	-	-	-	-
		Without pulse breakup	12,002	-	33	-	33	-	10	23
			Percent of pulses	-	0.27%	-	0.27%	-	-	-
		Free flow total	38,232	416	430	384	46	32	20	26
			Percent of pulses	1.09%	1.12%	1.00%	0.12%	0.08%	-	-
			Percent of pulse breakups	-	-	92.3%	-	-	-	-
		Conge-stion	With pulse breakup	9,963	169	179	157	22	12	22
	Percent of pulses			1.70%	1.80%	1.58%	0.22%	0.12%	-	-
	Percent of pulse breakups			-	-	92.9%	-	-	-	-
	Without pulse breakup		8,308	-	85	-	85	-	70	15
			Percent of pulses	-	1.02%	-	1.02%	-	-	-
	Conge- s-tion total		18,271	169	264	157	107	12	92	15
			Percent of pulses	0.92%	1.44%	0.86%	0.59%	0.07%	-	-
Percent of pulse breakups			-	-	92.9%	-	-	-	-	

TABLE 2 Comparison of our proposed algorithm against two previous algorithms for detecting pulse breakup events

Traffic condition	Status of data	Method	Total pulses	Actual pulse breakup	Suspected pulse breakup	Performance		
						Success	False positive	False negative
Free Flow	Pulse breakup	C&M	26,230	416	364	283	81	133
		CYN			1,159	279	880	137
		L&C			397	384	13	32
	Non-Pulse breakup	C&M	12,002	-	94	-	94	-
		CYN			430	-	430	-
		L&C			33	-	33	-
Conge- tion	Pulse breakup	C&M	9,963	169	53	49	4	120
		CYN			36	14	22	155
		L&C			179	157	22	12
	Non-Pulse breakup	C&M	8,308	-	61	-	61	-
		CYN			74	-	74	-
		L&C			85	-	85	-

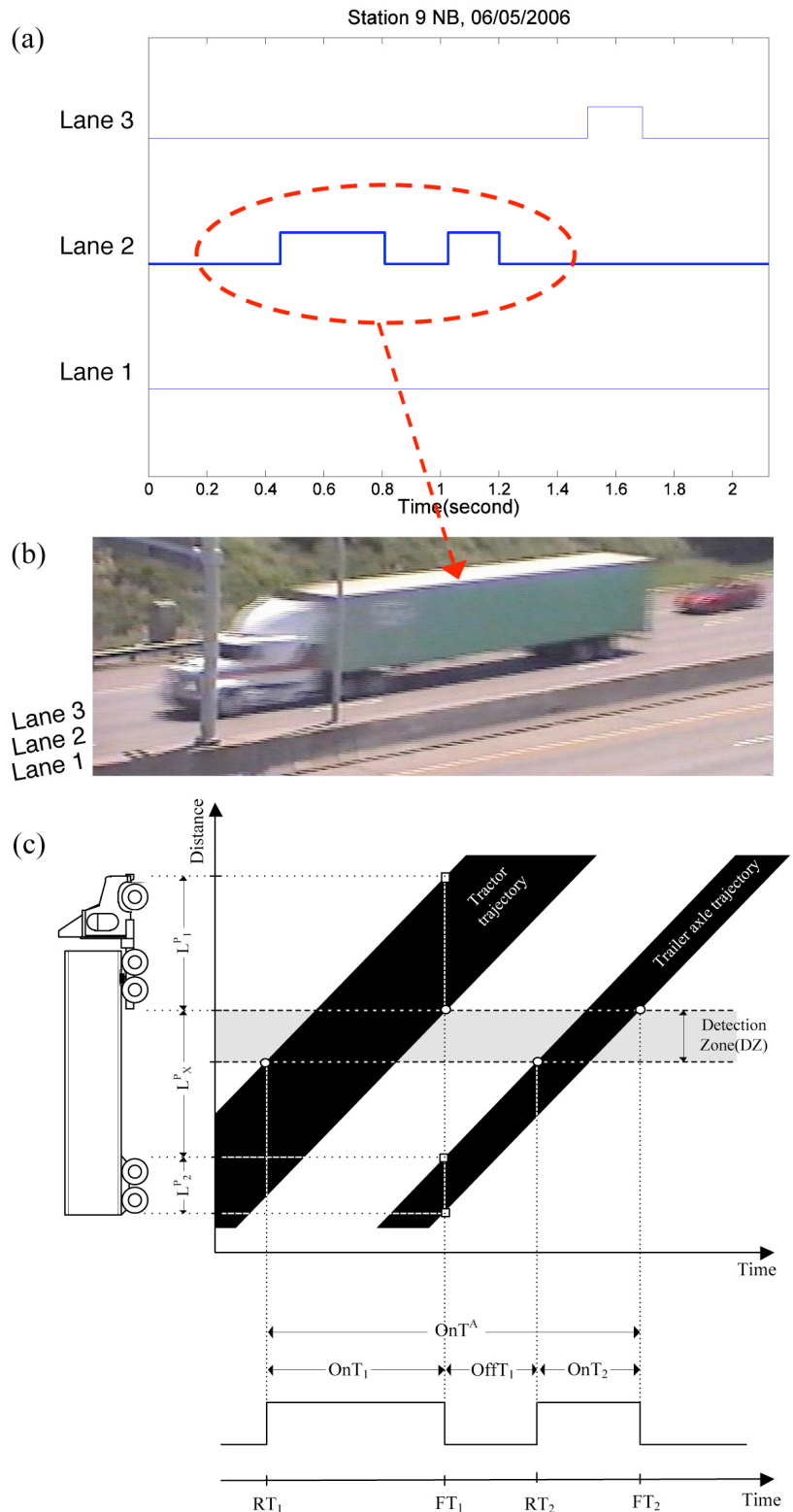


FIGURE 1 (a) A plot of transition pulses with pulse breakup recorded at station 9 northbound, (b) a concurrent video frame showing the two vehicles that gave rise to the three pulses, and (c) a time-space diagram illustrating a hypothetical example of pulse breakup and the associated detector's response.

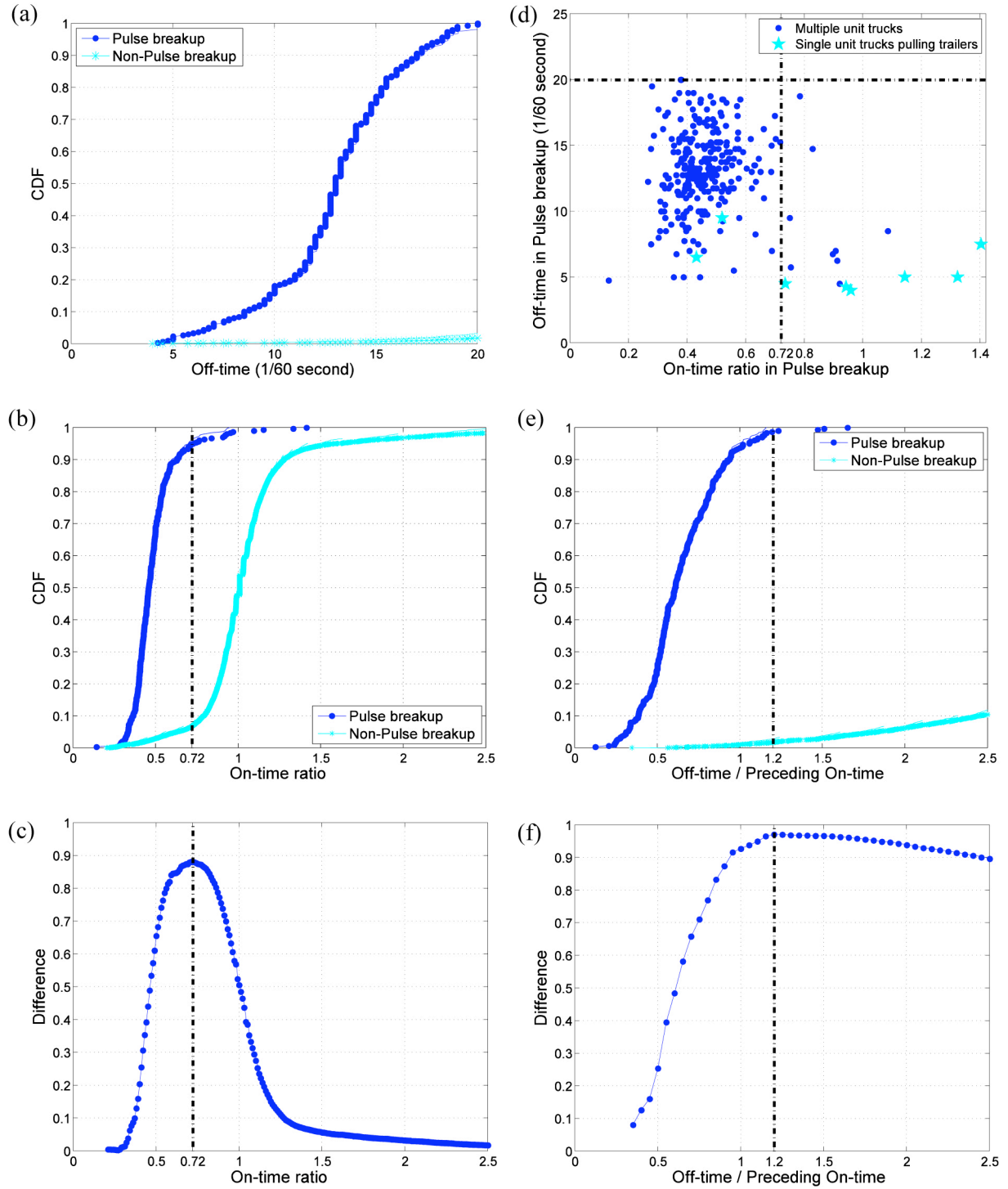


FIGURE 2 From the development dataset at station 9 northbound, (a) CDF of off-times from pulse breakup and from non-pulse breakup events, (b) CDF of the on-time ratio from pulse breakup and from non-pulse breakup events, (c) the difference between the two CDFs of the on-time ratio, (d) a scatter plot of off-time versus on-time ratio in pulse breakup events, (e) CDF of the ratio of off-time and preceding on-time from pulse breakup and from non-pulse breakup events, and (f) the difference between the two CDFs of the ratio of off-time and preceding on-time.

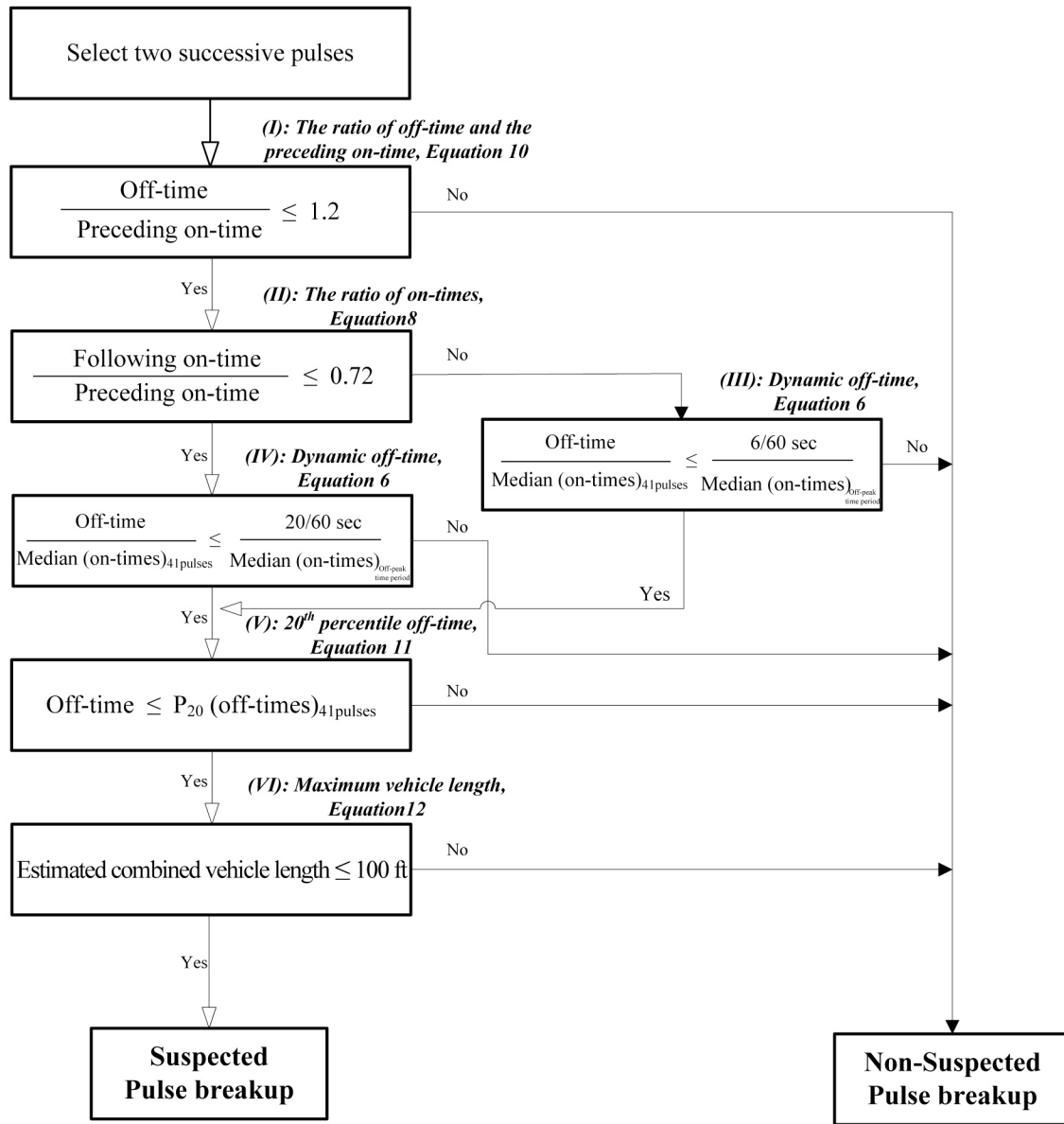


FIGURE 3 A flowchart of the algorithm to identify pulse breakup from single loop detectors.

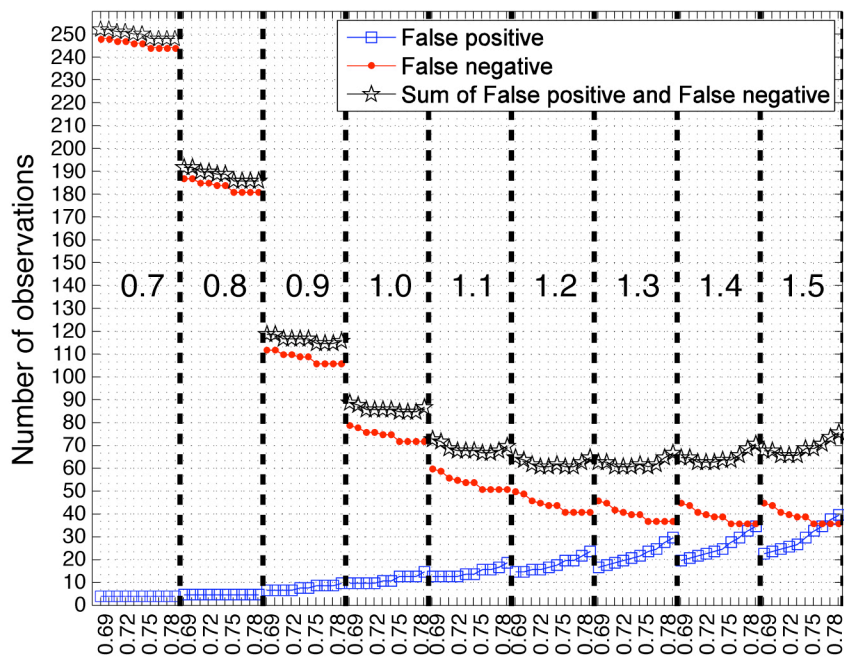


FIGURE 4 Sensitivity analysis of the performance of the pulse breakup detection algorithm relative to the combination of the on-time ratio threshold, and the ratio of off-time and preceding on-time threshold. The bold vertical delineations show the transition from one ratio of off-time and preceding on-time threshold to the next (indicated with large numbers on the figure), while the lighter vertical delineations show the steps between on-time ratio thresholds (indicated along the horizontal axis).